

## ENTANGLED-PHOTON STATE ENGINEERING

A. V. SERGIENKO, G. DI GIUSEPPE, M. ATATÜRE,  
B. E. A. SALEH, AND M. C. TEICH

*Quantum Imaging Laboratory, Department of Electrical & Computer Engineering  
and Department of Physics, Boston University, Boston, MA 02215, USA  
E-mail: AlexSerg@bu.edu*

We have studied experimentally and theoretically the hyper-entanglement of quantum states produced in the nonlinear process of spontaneous parametric downconversion. This simultaneous entanglement in several pairs of quantum variables (frequency, three-dimensional wave vector, and polarization) provides a significant resource for designing complex nonclassical states for quantum information processing and quantum measurement applications.

### 1 Introduction

In the nonlinear-optical process of spontaneous parametric downconversion (SPDC), in which a laser beam illuminates a nonlinear-optical crystal, pairs of photons are generated in a state that can be entangled<sup>1</sup> concurrently in frequency, momentum, and polarization. A significant number of experimental efforts designed to verify the entangled nature of such states have been carried out on states entangled in a *single* parameter, such as in energy,<sup>2</sup> momentum,<sup>3</sup> or polarization.<sup>4</sup> In general, the quantum state produced by SPDC is not factorizable into independently entangled single-parameter functions. Consequently any attempt to access one parameter is affected by the presence of the others. A common approach to quantum interferometry to date has been to choose a single entangled parameter of interest and eliminate the dependence of the quantum state on all other parameters. For example, when investigating polarization entanglement, spectral and spatial filtering are typically imposed in an attempt to restrict attention to polarization alone.

A more general approach to this problem is to consider and exploit the concurrent entanglement from the outset. In this approach, the observed quantum-interference pattern in one parameter, such as polarization, can be modified at will by controlling the dependence of the state on the other parameters, such as frequency and transverse wave vector. This strong interdependence has its origin in the nonfactorizability of the quantum state into product functions of the separate parameters.

We theoretically and experimentally study how the polarization quantum-interference pattern, presented as a function of relative temporal delay between the photons of an entangled pair, is modified by controlling the optical system through different kinds of spatial apertures. The effect of the spectral profile of the pump field is investigated by using both a continuous-wave and a pulsed laser to generate SPDC. The role of the spatial profile of the pump

field is also studied experimentally by restricting the pump-beam diameter at the face of the nonlinear crystal.

Spatial effects in Type-I SPDC have previously been investigated, typically in the context of imaging with spatially resolving detection systems.<sup>5,6</sup> The theoretical formalism presented here for Type-II SPDC is suitable for extension to Type-I in the presence of an arbitrary optical system and detection apparatus. Our study leads to a deeper physical understanding of multi-parameter entangled two-photon states and concomitantly provides a route for engineering these states for specific applications, including quantum information processing.

## 2 Multi-parameter Entangled-State Generation, Propagation, and Detection

**Generation.** By virtue of the relatively weak interaction in the nonlinear crystal, we consider the two-photon state generated within the confines of first-order time-dependent perturbation theory:

$$|\Psi^{(2)}\rangle \sim \frac{i}{\hbar} \int_{t_0}^t dt' \hat{H}_{\text{int}}(t') |0\rangle. \quad (1)$$

Here  $\hat{H}_{\text{int}}(t')$  is the interaction Hamiltonian,  $[t_0, t]$  is the duration of the interaction, and  $|0\rangle$  is the initial vacuum state. The interaction Hamiltonian governing this phenomenon is<sup>7</sup>

$$\hat{H}_{\text{int}}(t') \sim \chi^{(2)} \int_V d\mathbf{r} \hat{E}_p^{(+)}(\mathbf{r}, t') \hat{E}_o^{(-)}(\mathbf{r}, t') \hat{E}_e^{(-)}(\mathbf{r}, t') + \text{H.c.}, \quad (2)$$

where  $\chi^{(2)}$  is the second-order susceptibility and  $V$  is the volume of the nonlinear medium in which the interaction takes place. The operator  $\hat{E}_j^{(\pm)}(\mathbf{r}, t')$  represents the positive- (negative-) frequency portion of the  $j$ th electric-field operator, with the subscript  $j$  representing the pump ( $p$ ), ordinary ( $o$ ), and extraordinary ( $e$ ) waves at position  $\mathbf{r}$  and time  $t'$ , and H.c. stands for Hermitian conjugate. Because of the high intensity of the pump field it can be represented by a classical  $c$ -number, rather than as an operator, with an arbitrary spatiotemporal profile given by

$$E_p(\mathbf{r}, t) = \int d\mathbf{k}_p \tilde{E}_p(\mathbf{k}_p) e^{i\mathbf{k}_p \cdot \mathbf{r}} e^{-i\omega_p(\mathbf{k}_p)t}, \quad (3)$$

where  $\tilde{E}_p(\mathbf{k}_p)$  is the complex-amplitude profile of the field as a function of the wave vector  $\mathbf{k}_p$ .

We decompose the three-dimensional wave vector  $\mathbf{k}_p$  into a two-dimensional transverse wave vector  $\mathbf{q}_p$  and frequency  $\omega_p$ , so that Eq. (3) takes

the form

$$E_p(\mathbf{r}, t) = \int d\mathbf{q}_p d\omega_p \tilde{E}_p(\mathbf{q}_p; \omega_p) e^{i\kappa_p z} e^{i\mathbf{q}_p \cdot \mathbf{x}} e^{-i\omega_p t}, \quad (4)$$

where  $\mathbf{x}$  spans the transverse plane perpendicular to the propagation direction  $z$ . In a similar way the ordinary and extraordinary fields can be expressed in terms of the quantum-mechanical creation operators  $\hat{a}^\dagger(\mathbf{q}, \omega)$  for the  $(\mathbf{q}, \omega)$  modes as

$$\hat{E}_j^{(-)}(\mathbf{r}, t) = \int d\mathbf{q}_j d\omega_j e^{-i\kappa_j z} e^{-i\mathbf{q}_j \cdot \mathbf{x}} e^{i\omega_j t} \hat{a}_j^\dagger(\mathbf{q}_j, \omega_j), \quad (5)$$

where the subscript  $j = o, e$ . The longitudinal component of  $\mathbf{k}$ , denoted  $\kappa$ , can be written in terms of the  $(\mathbf{q}, \omega)$  pair as<sup>6,8</sup>

$$\kappa = \sqrt{\left[ \frac{n(\omega, \theta) \omega}{c} \right]^2 - |\mathbf{q}|^2}, \quad (6)$$

where  $c$  is the speed of light in vacuum,  $\theta$  is the angle between  $\mathbf{k}$  and the optical axis of the nonlinear crystal, and  $n(\omega, \theta)$  is the index of refraction in the nonlinear medium. Note that the symbol  $n(\omega, \theta)$  in Eq. (6) represents the extraordinary refractive index  $n_e(\omega, \theta)$  when calculating  $\kappa$  for extraordinary waves, and the ordinary refractive index  $n_o(\omega)$  for ordinary waves.

Substituting Eqs. (4) and (5) into Eqs. (1) and (2) yields the quantum state at the output of the nonlinear crystal:

$$|\Psi^{(2)}\rangle \sim \int d\mathbf{q}_o d\mathbf{q}_e d\omega_o d\omega_e \Phi(\mathbf{q}_o, \mathbf{q}_e; \omega_o, \omega_e) \hat{a}_o^\dagger(\mathbf{q}_o, \omega_o) \hat{a}_e^\dagger(\mathbf{q}_e, \omega_e) |0\rangle, \quad (7)$$

with

$$\Phi(\mathbf{q}_o, \mathbf{q}_e; \omega_o, \omega_e) = \tilde{E}_p(\mathbf{q}_o + \mathbf{q}_e; \omega_o + \omega_e) L \text{sinc}\left(\frac{L\Delta}{2}\right) e^{-i\frac{L\Delta}{2}}, \quad (8)$$

where  $L$  is the thickness of the crystal and  $\Delta = \kappa_p - \kappa_o - \kappa_e$  where  $\kappa_j$  ( $j = p, o, e$ ) is related to the indices  $(\mathbf{q}_j, \omega_j)$  via relations similar to Eq. (6). The nonseparability of the function  $\Phi(\mathbf{q}_o, \mathbf{q}_e; \omega_o, \omega_e)$  in Eqs. (7) and (8), recalling (6), is the hallmark of *concurrent* multi-parameter entanglement.

**Propagation.** Propagation of the downconverted light between the planes of generation and detection is characterized by the transfer function of the optical system. The biphoton probability amplitude<sup>7</sup> at the space-time coordinates  $(\mathbf{x}_A, t_A)$  and  $(\mathbf{x}_B, t_B)$  where detection takes place is defined by

$$A(\mathbf{x}_A, \mathbf{x}_B; t_A, t_B) = \langle 0 | \hat{E}_A^{(+)}(\mathbf{x}_A, t_A) \hat{E}_B^{(+)}(\mathbf{x}_B, t_B) | \Psi^{(2)} \rangle. \quad (9)$$

The explicit forms of the quantum operators using the transfer function  $\mathcal{H}_{ij}$  ( $i = A, B$  and  $j = e, o$ ) describing the propagation of a  $(\mathbf{q}, \omega)$  mode from the nonlinear-crystal output plane to the detection plane can be found in Ref. 6. By choosing optical systems with explicit forms of the functions  $\mathcal{H}_{Ae}$ ,  $\mathcal{H}_{Ao}$ ,

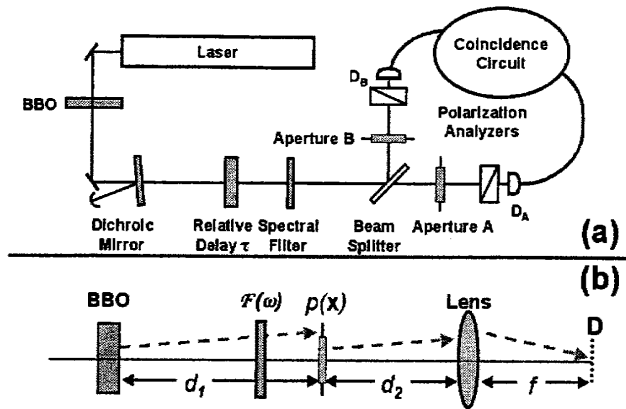


Figure 1. (a) Schematic of the experimental setup for observation of quantum interference using type-II collinear SPDC. (b) Detail of the path from the crystal output plane to the detector input plane.  $\mathcal{F}(\omega)$  represents an (optional) filter transmission function,  $p(x)$  represents an aperture function, and  $f$  is the focal length of the lens.

$\mathcal{H}_{Be}$ , and  $\mathcal{H}_{Bo}$ , the overall biphoton probability amplitude is constructed as desired.

**Detection.** The formulation of the detection process requires some knowledge of the detection apparatus. Slow detectors, for example, impart temporal integration whereas detectors of finite area impart spatial integration. One extreme case is realized when the temporal response of a *point* detector is spread negligibly with respect to the characteristic time scale of SPDC, namely the inverse of downconversion bandwidth. In this limit the coincidence rate reduces to

$$R = |A(\mathbf{x}_A, \mathbf{x}_B; t_A, t_B)|^2. \quad (10)$$

On the other hand, quantum-interference experiments typically make use of slow *bucket* detectors. Under these conditions, the coincidence count rate  $R$  is readily expressed in terms of the biphoton probability amplitude as

$$R = \int dx_A dx_B dt_A dt_B |A(\mathbf{x}_A, \mathbf{x}_B; t_A, t_B)|^2. \quad (11)$$

### 3 Multi-parameter Entangled-State Manipulation

We now apply this formalism<sup>9</sup> to a specific configuration of entangled-photon quantum interferometer illustrated in Fig. 1.

**Quantum Interference with Shifted-Ring Apertures.** In all existing experimental reports using parametric downconversion the optical elements in the system are placed concentrically about the longitudinal ( $z$ ) axis.

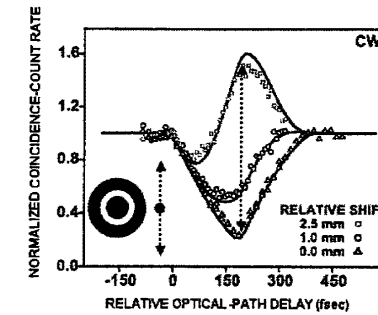


Figure 2. Normalized coincidence-count rate as a function of the relative optical-path delay, for an annular aperture (internal and external diameters of 2 and 4 mm, respectively) in one of the arms of the interferometer in the configuration of Fig. 1. A 7 mm circular aperture is placed in the other arm. The data were obtained using a 351 nm cw pump and no spectral filters. The symbols are experimental results for different relative shifts of the annulus along the direction of the optical axis of the crystal (vertical). The solid curves are the theoretical plots without any fitting parameters.

In this condition, the sole aperture before the beam splitter, as shown in Fig. 1(a), yields the same transfer function as two identical apertures placed in each arm after the beam splitter. We demonstrated experimentally that the observed quantum-interference pattern is also sensitive to a *relative shift* of the apertures in the transverse plane. This extra factor provides yet another degree of control on the quantum-interference pattern for a given aperture form. This new feature provides us with a great deal of flexibility in designing and manipulating polarization entangled quantum states.

Given the experimental setup shown in Fig. 1 with an annular aperture in arm A and a 7 mm circular aperture in arm B, we obtained the quantum-interference patterns shown in Fig. 2. The annular aperture used had an outer diameter of  $b = 4$  mm and an inner diameter of  $a = 2$  mm. The symbols give the experimental results for various values of the relative shift  $|s_A - s_B|$ , as denoted in the legend. Note that as in the case of the shifted slit, the interference pattern displays a peak rather than the familiar triangular dip usually expected in this type of experiment. Traditionally this effect can be achieved only by polarization analyzer rotation.

### 4 Conclusion

In summary, we observe that the multi-parameter entangled nature of the two-photon state generated by SPDC allows transverse spatial effects to play a role in polarization-based quantum-interference experiments. The interfer-

ence patterns generated in these experiments are, as a result, governed in part by the profiles of the apertures in the optical system, which admit wave vectors in specified directions. The observed quantum-interference pattern in one feature, such as polarization (Bell-states), can be modified by controlling the dependence of the state on the other parameters, such as frequency and transverse wave vector. This strong interdependence has its origin in the nonfactorizability of the quantum state into product functions of the separate forms of entanglement. We theoretically and experimentally show how the polarization Bell-state quantum-interference pattern can be modified at will by controlling the optical system through manipulation of its spatial and temporal characteristics. Our study provides a route for engineering hyper-entangled states to be used in quantum-information and quantum-measurement technologies.

## References

1. E. Schrödinger, *Naturwissenschaften* **23**, 807 (1935); **23**, 823 (1935); **23**, 844 (1935) [Translation: J. D. Trimmer, *Proc. Am. Phil. Soc.* **124**, 323 (1980); reprinted in *Quantum Theory and Measurement*, edited by J. A. Wheeler and W. H. Zurek (Princeton University Press, Princeton, 1983)].
2. C. K. Hong, Z. Y. Ou, and L. Mandel, *Phys. Rev. Lett.* **59**, 2044 (1987); P. G. Kwiat, A. M. Steinberg, and R. Y. Chiao, *Phys. Rev. A* **47**, R2472 (1993).
3. J. G. Rarity and P. R. Tapster, *Phys. Rev. Lett.* **64**, 2495 (1990).
4. Z. Y. Ou and L. Mandel, *Phys. Rev. Lett.* **61**, 50 (1988); Y. H. Shih and C. O. Alley, *Phys. Rev. Lett.* **61**, 2921 (1988); Y. H. Shih and A. V. Sergienko, *Phys. Lett. A* **191**, 201 (1994); P. G. Kwiat, K. Mattle, H. Weinfurter, A. Zeilinger, A. V. Sergienko, and Y. H. Shih, *Phys. Rev. Lett.* **75**, 4337 (1995).
5. A. Joobeur, B. E. A. Saleh, and M. C. Teich, *Phys. Rev. A* **50**, 3349 (1994); C. H. Monken, P. H. Souto Ribeiro, and S. Pádua, *Phys. Rev. A* **57**, 3123 (1998); B. E. A. Saleh, A. Joobeur, and M. C. Teich, *Phys. Rev. A* **57**, 3991 (1998).
6. B. E. A. Saleh, A. F. Abouraddy, A. V. Sergienko, and M. C. Teich, *Phys. Rev. A* **62**, 043816 (2000).
7. D. N. Klyshko, *Photons and Nonlinear Optics* (Gordon and Breach Science Publishers, New York, 1988).
8. T. B. Pittman, D. V. Strekalov, D. N. Klyshko, M. H. Rubin, A. V. Sergienko, and Y. H. Shih, *Phys. Rev. A* **53**, 2804 (1996).
9. M. Atatüre, G. Di Giuseppe, M. D. Shaw, A. V. Sergienko, B. E. A. Saleh, and M. C. Teich, *Phys. Rev. A* **66**, 023822 (2002).